

---

# Federated Unsupervised Semantic Segmentation

---

**Evangelos Charalampakis\***

Department of Informatics  
Aristotle University of Thessaloniki  
Thessaloniki, 54124  
charevan@csd.auth.gr

**Vasileios Mygdalis**

Department of Informatics  
Aristotle University of Thessaloniki  
Thessaloniki, 54124  
mygdalisv@csd.auth.gr

**Ioannis Pitas**

Department of Informatics  
Aristotle University of Thessaloniki  
Thessaloniki, 54124  
pitas@csd.auth.gr

## Abstract

This work explores the application of Federated Learning (FL) in Unsupervised Semantic image Segmentation (USS). Recent USS methods extract pixel-level features using frozen visual foundation models and refine them through self-supervised objectives that encourage semantic grouping. These features are then grouped to semantic clusters to produce segmentation masks. Extending these ideas to federated settings requires feature representation and cluster centroid alignment across distributed clients—an inherently difficult task under heterogeneous data distributions in the absence of supervision. To address this, we propose **FUSS** (Federated Unsupervised image Semantic Segmentation) which is, to our knowledge, the first framework to enable fully decentralized, label-free semantic segmentation training. FUSS introduces novel federation strategies that promote global consistency in feature and prototype space, jointly optimizing local segmentation heads and shared semantic centroids. Experiments on both benchmark and real-world datasets, including binary and multi-class segmentation tasks, show that FUSS consistently outperforms local-only client trainings as well as extensions of classical FL algorithms under varying client data distributions. To support reproducibility, full code will be released upon manuscript acceptance.

## 1 Introduction

Semantic image segmentation is a fundamental computer vision task, serving as a core component of visual perception systems deployed in safety-critical applications like autonomous driving [Tang et al., 2022], industrial inspection [Psarras et al., 2024], and medical diagnostics [Chen et al., 2024]. Unsupervised Semantic Segmentation (USS) has emerged as a family of methods that do not require the notoriously famous pixel-wise annotations. Recent USS approaches employ pretrained Convolutional Neural Networks (CNNs) [He et al., 2016] or Vision Foundation Models (VFM) [Caron et al., 2021, Dosovitskiy et al., 2020] to extract pixel-wise feature embeddings. These representations are fed into learnable segmentation heads that are fine-tuned through self-supervised learning objectives such as contrastive losses [Guerhazi et al., 2024], energy minimization [Hamilton et al., 2022], or eigenvector alignment [Kim et al., 2024]. Unsupervised segmentation is ultimately achieved by simply clustering the learned representations.

---

\*Corresponding author.

In safety-critical domains, strict privacy constraints on data storage and sharing introduce significant challenges in effectively training robust and generalizable DNN-based image segmentation models. To this end, Federated Learning (FL) [McMahan et al., 2017, Caldarola et al., 2022, Gong et al., 2021, Fantauzzo et al., 2022] has emerged as a promising paradigm that enables collaborative model training with decentralized data. Perhaps the most recognizable FL method is FedAvg McMahan et al. [2017], a method that simply aggregates the weights between federation clients. The simplicity and elegance of FedAvg render it applicable to almost every supervised or unsupervised training [Lubana et al., 2022, Liao et al., 2024] scenario, consisting FedAvg the standard benchmark in most FL applications.

In semantic image segmentation, FL has only been applied in the supervised training case [Miao et al., 2023]. The special challenge of federated semantic image segmentation is that data heterogeneity across clients is coupled with large within-class variance due to fine-graining (i.e., pixel regions of semantically similar objects may differ significantly). Supervised training objectives [Miao et al., 2023] are known to alleviate such issues, since they can "push" the representations of similar objects to the same target values across all clients. Nevertheless, these questions remain open and unexplored for the Federated Unsupervised Semantic Segmentation problem, where such supervised signals simply cannot be obtained.

To bridge this gap, we propose **FUSS** (Federated Unsupervised image Semantic Segmentation), a novel framework for collaborative unsupervised training of image segmentation DNN models in decentralized settings. FUSS addresses both data annotation scarcity and privacy constraints by enabling clients to jointly learn DNN segmentation heads and class prototypes using unsupervised objectives and communication-efficient parameter exchanges.

The key contributions of this paper are summarized as follows:

- We identify a fundamental gap in current federated image segmentation literature, namely, its reliance on annotated image data, which limits applicability in privacy-constrained data settings.
- We introduce FUSS, a label-free federated learning framework that combines unsupervised representation learning with clustering-based semantic aggregation to enable efficient federated image segmentation training without human supervision.
- We develop a novel aggregation strategy, namely **Federated Centroid Clustering (FedCC)**, tailored to federated unsupervised segmentation. FedCC supports joint optimization of client-specific segmentation heads and global alignment of semantic class prototypes, enabling effective end-to-end training in decentralized settings.
- We conduct extensive experiments on real-world image semantic segmentation datasets, demonstrating that FUSS combined with FedCC consistently outperforms local DNN training and extensions of traditional FL aggregation strategies in fully unsupervised i.i.d and non-i.i.d federated scenarios, while preserving scalability and privacy.

## 2 Unsupervised image Semantic Segmentation

USS aims to segment images into semantically coherent regions without requiring human labels. Recent methods follow a common two-stage pipeline: a) extract dense pixel-level feature embeddings using pretrained self-supervised models, and b) optimize over these representations using unsupervised objectives to produce segmentation masks.

Formally, given an unlabeled image dataset  $\mathcal{D} = \{\mathbf{X}_i \in \mathbb{R}^{H \times W \times 3} \mid i = 1, \dots, N\}$ , the goal of USS is to estimate a segmentation mask  $\hat{\mathbf{Y}}_i \in \{0, 1\}^{H \times W \times |\mathcal{C}|}$  for each image, where  $\mathcal{C}$  denotes the set of semantic regions or latent classes to be discovered in the data. In the absence of ground-truth labels, the value of  $|\mathcal{C}|$  is assumed to be known and remains fixed.

**Feature extraction.** Let  $E$  denote a pretrained DNN encoder that maps an image  $\mathbf{X}_i$  to a spatial feature tensor  $\mathbf{H}_i = E(\mathbf{X}_i)$ , with  $\mathbf{H}_i \in \mathbb{R}^{H \times W \times D}$ . Each location  $(h, w)$  in  $\mathbf{H}_i$  corresponds to a  $D$ -dimensional embedding capturing local semantic context.

To enable clustering, the encoder must produce similar features for pixels depicting the same semantic object, while allowing different objects to be distinguishable. We define a general similarity function:

$$s(\mathbf{H}^{(h,w)}, \mathbf{H}^{(m,n)}) = \phi\left(\psi(\mathbf{H}^{(h,w)}, \mathbf{H}^{(m,n)})\right), \quad (1)$$

where  $\psi : \mathbb{R}^D \times \mathbb{R}^D \rightarrow \mathbb{R}$  is a base similarity metric (e.g., cosine similarity), and  $\phi : \mathbb{R} \rightarrow \mathbb{R}$  is an optional normalization function. Higher values of  $s$  indicate stronger semantic affinity between pixel representations, supporting clustering-based label discovery.

To guide the encoder  $E$  towards learning semantically coherent pixel-wise representations, contrastive objectives are typically employed [Caron et al., 2021]. The resulting loss functions promote intra-object compactness by increasing the similarity among perceptually related pixels, while simultaneously encouraging inter-object separability by reducing similarity between unrelated regions.

We formalize this principle with a general contrastive loss template defined over feature similarities:

$$\mathcal{L}_{\text{contrast}} = \sum_{(p,q) \in \mathcal{P}} \left[ -s(\mathbf{H}^{(p)}, \mathbf{H}^{(q)}) + \frac{1}{|\mathcal{N}(p)|} \sum_{r \in \mathcal{N}(p)} s(\mathbf{H}^{(p)}, \mathbf{H}^{(r)}) \right], \quad (2)$$

where  $\mathcal{P}$  denotes the set of positive pixel pairs in the feature map  $\mathbf{H}$  and  $\mathcal{N}(p)$  the set of negatives for anchor  $p$ . This formulation encourages perceptually related features to be close in the embedding space, while distancing unrelated ones. Once such discriminative feature representations are obtained, the next step involves grouping them into semantically consistent regions via clustering.

**Pixel feature clustering.** Following feature extraction, the second stage of the USS pipeline involves grouping pixel-level feature vectors into  $|\mathcal{C}|$  distinct clusters, each corresponding to a semantic region. We define a matrix  $\mathbf{M} \in \mathbb{R}^{|\mathcal{C}| \times D}$ , where each row  $\mathbf{m}_c$  is a cluster centroid representing a semantic prototype for the  $c$ -th region or object class. To associate pixel embeddings with cluster prototypes, we first reshape the encoder output  $\mathbf{H}_i \in \mathbb{R}^{H \times W \times D}$  into a matrix  $\tilde{\mathbf{H}}_i \in \mathbb{R}^{(HW) \times D}$ , where each row corresponds to the feature vector of a spatial location. We then compute the similarity matrix via inner product:

$$\tilde{\mathbf{P}}_i = \tilde{\mathbf{H}}_i \mathbf{M}^\top, \quad (3)$$

where  $\tilde{\mathbf{P}}_i \in \mathbb{R}^{(HW) \times |\mathcal{C}|}$  contains the unnormalized similarity scores between pixel features and centroids. To maintain consistency with the spatial structure of the input image, we reshape the result back into a tensor  $\mathbf{P}_i \in \mathbb{R}^{H \times W \times |\mathcal{C}|}$ . Each element  $\mathbf{P}_i^{(h,w,c)} \in \mathbb{R}$  measures the similarity between feature  $\mathbf{H}_i^{(h,w)}$  and centroid  $\mathbf{m}_c$ . The segmentation mask  $\hat{\mathbf{Y}}_i$  is then produced by assigning each pixel to its most similar cluster:

$$\hat{\mathbf{Y}}_i^{(h,w,c)} = \begin{cases} 1, & \text{if } c = \arg \max_{c'} \mathbf{P}_i^{(h,w,c')}, \\ 0, & \text{otherwise.} \end{cases} \quad (4)$$

This operation assigns each pixel to its most semantically similar cluster centroid, yielding a one-hot encoded segmentation mask.

The predicted masks depend critically on the quality of the centroids  $\mathbf{m}_c$ , which must reflect meaningful semantic structure in the embedding space. However, in USS, where all pixels across the dataset  $\mathcal{D}$  are treated as clustering targets, full-dataset pixel feature extraction and traditional clustering (e.g., k-means) is computationally prohibitive.

Instead, the centroid matrix  $\mathbf{M}$  is initialized randomly and incrementally optimized with each mini-batch of extracted features [MacQueen, 1967]. The goal is for pixel representations assigned to the same centroid to be similar, while different centroids remain well-separated. This is typically achieved by minimizing intra-cluster variance and penalizing inter-cluster similarity:

$$\mathcal{L}_{\text{cluster}} = \underbrace{\sum_{i,h,w} \left\| \mathbf{H}_i^{(h,w)} - \mathbf{m}_{a_i^{(h,w)}} \right\|^2}_{\text{intra-cluster variance}} + \lambda \cdot \underbrace{\sum_{c \neq c'} s(\mathbf{m}_c, \mathbf{m}_{c'})}_{\text{inter-cluster similarity}}, \quad (5)$$

where  $a_i^{(h,w)}$  denotes the index of the centroid assigned to pixel  $(h,w)$ , and  $\lambda > 0$  controls the trade-off between compactness and inter-cluster separation. This objective encourages compact, well-separated prototypes and enables stable pixel-to-region assignments in the absence of ground truth labels.

### 3 Federated Unsupervised Semantic Segmentation (FUSS)

FUSS extends the standard Federated Learning (FL) paradigm [McMahan et al., 2017, Li et al., 2020, 2021] to the unsupervised semantic segmentation setting, where clients must collaboratively train segmentation models without any labeled data or data sharing. Let  $\mathcal{K}$  denote the set of participating clients, each indexed by  $k$ . Each client holds a private unlabeled dataset  $\mathcal{D}_k = \{\mathbf{X}_{k_i} \in \mathbb{R}^{H \times W \times 3} \mid i = 1, \dots, N_k\}$ , where  $N_k$  is the number of local images. The global dataset is  $\mathcal{D} = \bigcup_{k \in \mathcal{K}} \mathcal{D}_k$ , with total size  $N = \sum_{k \in \mathcal{K}} N_k$ .

Each client independently trains a local encoder  $E_k$  with parameters  $\theta_{E_k}$  and maintains a local centroid matrix  $\mathbf{M}_k \in \mathbb{R}^{|\mathcal{C}| \times D}$ . Local training is performed using the client’s private data and unsupervised objectives, and periodically, clients transmit their updated encoder parameters and centroids to a central server. The server aggregates these updates and broadcasts global model parameters  $\bar{\theta}_E$  and aligned centroid matrix  $\mathbf{M}$  back to all clients.

Unlike traditional FL setups, FUSS must ensure consistency not only in feature extraction but also in semantic clustering. Aligning the learned prototypes  $\mathbf{M}_k$  across clients is nontrivial, as potential local data heterogeneity can induce variation in learned feature spaces and disrupt semantic alignment. To mitigate the adverse effects of data heterogeneity and class imbalance during local representation learning, FUSS leverages recent advances in vision foundation models (VFMs) such as DINO [Caron et al., 2021], which produce semantically meaningful pixel embeddings without supervision, that coarsely align semantically similar regions even across unseen classes. Due to space constraints, a visual representation of the FUSS framework is deferred to Appendix A.

#### 3.1 Local training

Following the centralized USS training of [Hamilton et al., 2022], each client in FUSS is initialized with a frozen VFM encoder, enabling efficient and stable local learning. This choice aligns with recent trends in efficient FL adaptation [Wang et al., 2024], though FUSS takes a simpler approach: by freezing the backbone of the encoder entirely, each client performs one-time feature extraction over its local dataset, and optimizes and transmits only a segmentation head  $S_k$  and the centroid matrix  $\mathbf{M}_k$ . This eliminates the need for layer scheduling or repeated backward passes, enabling streamlined training even in resource-constrained settings.

Specifically, let  $E_{\text{VFM}}(\cdot, \theta_{\text{VFM}})$  denote a pretrained backbone that produces intermediate feature maps:

$$\mathbf{Z}_{k_i} = E_{\text{VFM}}(\mathbf{X}_{k_i}, \theta_{\text{VFM}}) \in \mathbb{R}^{H \times W \times D'},$$

and  $S_k(\cdot, \theta_{S_k})$  a lightweight, trainable projection head that maps these features to a segmentation embedding space:

$$\mathbf{H}_{k_i} = S_k(\mathbf{Z}_{k_i}, \theta_{S_k}) \in \mathbb{R}^{H \times W \times D}.$$

To optimize the segmentation head, since  $D > D'$  FUSS, instead of a loss in the form of Eq. 2, adopts a correspondence distillation loss that encourages semantic consistency across images, across features projected in different dimensions. Given feature tensors  $\mathbf{Z}_{k_i}$  and  $\mathbf{Z}_{k_j}$  from two images, we define a cosine similarity tensor:

$$\mathbf{A}_{k_i,j}^{(h,w,m,n)} := s_{\cos}(\mathbf{Z}_{k_i}^{(h,w)}, \mathbf{Z}_{k_j}^{(m,n)}),$$

and similarly for the projected embeddings:

$$\mathbf{Q}_{k_i,j}^{(h,w,m,n)} := s_{\cos}(\mathbf{H}_{k_i}^{(h,w)}, \mathbf{H}_{k_j}^{(m,n)}).$$

The projection head is trained to align  $\mathbf{Q}_{k_i,j}$  with  $\mathbf{A}_{k_i,j}$  using the following loss:

$$\mathcal{L}_{\text{corr}}(\mathbf{X}_{k_i}, \mathbf{X}_{k_j}) = - \sum_{h,w,m,n} \left( \mathbf{A}_{k_i,j}^{(h,w,m,n)} - b \right) \mathbf{Q}_{k_i,j}^{(h,w,m,n)}, \quad (6)$$

where  $b \in \mathbb{R}$  suppresses weak correspondences. This objective encourages the segmentation head to enhance semantic coherence already present in the VFM features. After each parameter update minimizing Eq. 6, the extracted features are utilized in Eq. 5 to update the local centroid matrix  $\mathbf{M}_k$ , with the final local loss:

$$\mathcal{L}_{\text{local}} = \mathcal{L}_{\text{corr}} + \mathcal{L}_{\text{cluster}}. \quad (7)$$

---

**Algorithm 1:** Federated Unsupervised Semantic Segmentation (FUSS)

---

**Input** : Clients  $\mathcal{K}$ , pretrained VFM  $E_{\text{VFM}}$ , projection head  $S_k$ , centroids  $\mathbf{M}_k$ , rounds  $R$

**Output** : Global segmentation head  $\bar{\theta}_S$  and centroids  $\bar{\mathbf{M}}$

```
for  $r = 1$  to  $R$  do
  foreach client  $k \in \mathcal{K}$  in parallel do
    Receive  $(\bar{\theta}_S, \bar{\mathbf{M}})$  from server
    Initialize  $\theta_{S_k} \leftarrow \bar{\theta}_S, \mathbf{M}_k \leftarrow \bar{\mathbf{M}}$ 
    for each local step do
      Sample mini-batch  $\{\mathbf{X}_{k_i}\}$ 
      Extract features:  $\mathbf{Z}_{k_i} = E_{\text{VFM}}(\mathbf{X}_{k_i})$ 
       $\mathbf{H}_{k_i} = S_k(\mathbf{Z}_{k_i}, \theta_{S_k})$ 
      Compute  $\mathcal{L}_{\text{corr}}, \mathcal{L}_{\text{cluster}}$ 
      Update  $\theta_{S_k}, \mathbf{M}_k$ 
    Send  $(\theta_{S_k}, \mathbf{M}_k)$  to server
  Server aggregates into  $(\bar{\theta}_S, \bar{\mathbf{M}})$ 
  Server broadcasts parameters to all clients
```

---

### 3.2 Federated Aggregation Strategies

A major contribution of this work is the design of novel aggregation strategies for federated unsupervised semantic segmentation. In FUSS, each client transmits a local segmentation head  $\theta_{S_k}$  and a centroid matrix  $\mathbf{M}_k$ , representing learned class prototypes. Existing FL methods are ill-suited for this setting, as they were not designed to aggregate both feature extractors and latent semantic clusters in the absence of labels.

To address this gap, we propose a suite of aggregation mechanisms tailored to the dual objective of FUSS: maintaining feature consistency across clients while achieving global alignment of semantic prototypes. These include principled adaptations of classical methods as well as entirely new strategies, specifically formulated to support end-to-end, label-free training under both i.i.d. and non-i.i.d. client distributions. To our knowledge, this is the first work to explicitly formulate aggregation objectives that jointly optimize pixel-level representation alignment and global semantic clustering in a fully federated, unsupervised semantic segmentation setting.

#### 3.2.1 Extended Federated Averaging

We adapt the canonical Federated Averaging algorithm [McMahan et al., 2017] to our setting by aggregating both the segmentation head and the centroid matrix. While standard FedAvg aggregates encoder weights, it does not account for latent class prototypes — a critical element in FUSS. Let  $\theta_{S_k}$  denote the segmentation head parameters and  $\mathbf{M}_k \in \mathbb{R}^{|\mathcal{C}| \times D}$  the centroid matrix from client  $k$ . The aggregated global parameters are:

$$\bar{\theta}_S = \sum_{k \in \mathcal{K}} \alpha_k \theta_{S_k}, \quad (8)$$

$$\bar{\mathbf{M}} = \sum_{k \in \mathcal{K}} \alpha_k \mathbf{M}_k, \quad (9)$$

where  $\alpha_k = \frac{N_k}{N}$  reflects client weighting based on local dataset size, or  $\alpha_k = \frac{1}{|\mathcal{K}|}$  for uniform aggregation. This extension serves as a simple yet effective baseline for jointly aligning learned features and semantic prototypes across clients.

#### 3.2.2 Centroid Clustering for Prototype Alignment (FedCC)

While FedAvg serves as a simple baseline, it implicitly assumes that each centroid index  $c$  corresponds to the same semantic class across clients. This assumption fails in unsupervised settings, where clients observe unknown subsets of the global class distribution and learn centroids in arbitrary orders. As a result, averaging centroids  $\mathbf{m}_c^i$  and  $\mathbf{m}_c^j$  from different clients may collapse distinct semantics

into uninformative or ambiguous prototypes. This motivates a need for aggregation strategies that reason explicitly over the structure of the centroid space rather than relying on index alignment.

We propose **Federated Centroid Clustering (FedCC)**, a family of novel aggregation strategies that cluster the union of local prototypes across clients. Rather than assuming consistent object-to-centroid mappings across clients, FedCC clusters the pooled centroids globally—treating all received centroids as unordered semantic candidates. This strategy remains agnostic to local class semantics and promotes emergent alignment through global structure discovery in prototype space.

To construct the new global prototype matrix  $\bar{\mathbf{M}}$ , we pool all centroids across clients:

$$\mathbf{m}_{\text{pool}} = \bigcup_{k \in \mathcal{K}} \{\mathbf{m}_{k_c} \mid c = 1, \dots, |\mathcal{C}|\} \in \mathbb{R}^{(|\mathcal{K}| \cdot |\mathcal{C}|) \times D}. \quad (10)$$

We now describe two strategies for deriving  $\bar{\mathbf{M}}$  from this pool, where each row  $\bar{\mathbf{m}}_c$  represents the final global semantic centroid for class  $c$ .

**(a) FedCC -  $k$ Means Clustering.** In this variant, the server applies  $k$ -means clustering to  $\mathcal{M}_{\text{pool}}$ , using  $C = |\mathcal{C}|$  clusters to match the number of semantic prototypes. Each cluster center is used to construct a row in the updated global prototype matrix:

$$\bar{\mathbf{m}}_c = \frac{1}{|\mathcal{C}_c|} \sum_{\mathbf{m} \in \mathcal{C}_c} \mathbf{m}, \quad \forall c = 1, \dots, |\mathcal{C}|, \quad (11)$$

where  $\mathcal{C}_c \subset \mathcal{M}_{\text{pool}}$  denotes the set of centroids assigned to cluster  $c$ . This method promotes alignment by grouping structurally similar client prototypes in the embedding space, even when local class semantics are mismatched.

**(b) FedCC - Maximin Prototype Selection.** To encourage semantic diversity, we propose a maximin selection strategy. Starting with a randomly chosen centroid, each subsequent prototype is selected to maximize its minimum distance to all previously selected ones:

$$\bar{\mathbf{m}}_c = \arg \max_{\mathbf{m} \in \mathcal{M}_{\text{pool}}} \min_{c' < c} \|\mathbf{m} - \bar{\mathbf{m}}_{c'}\|_2. \quad (12)$$

This strategy avoids prototype collapse and enforces maximal separation in the feature space, which is particularly beneficial when classes appear as small objects or are dominated by background regions—conditions that often yield overlapping pixel-level representations.

In both variants,  $\bar{\theta}_S$  is updated via Eq. (8), and the resulting pair  $(\bar{\theta}_S, \bar{\mathbf{M}})$  is broadcast to all clients. The two variants of FedCC serve complementary goals: FedCC- $k$ Means promotes semantic consensus by averaging structurally similar centroids across clients, while FedCC-Maximin promotes semantic diversity, selecting centroids that span the prototype space. The former is suitable when clients share overlapping classes with misaligned feature clusters, whereas the latter guards against prototype collapse class-imbalanced settings.

## 4 Experiments

We evaluate FUSS under realistic federated scenarios involving decentralized, unlabeled datasets, without access to class labels or distributional metadata. Our goal is to measure segmentation performance under privacy-preserving constraints. Algorithm 1 outlines the full FUSS training framework.

### 4.1 Experimental Setup

The proposed FUSS framework is evaluated under a client-server federated learning paradigm, where each client independently trains on private, non-disclosable image datasets and periodically participates in server-coordinated model aggregation rounds. Training is conducted for simulated federations with different numbers of clients, with 10 global aggregation rounds. In each round, all clients perform local training over their datasets and return updated parameters and centroids for aggregation. Global validation is performed centrally on a held-out set.

We conduct experiments on the following benchmarks: Cityscapes [Cordts et al., 2016], a 1/21 subsampled version of CocoStuff [Caesar et al., 2018], and a private industrial dataset referred to as **IPS (Industrial Pipeline Segmentation)**.

Cityscapes is used to simulate a cross-silo federation: we reserve all samples from three cities for validation, and partition the remaining cities among clients. Depending on the federation size (3, 6, or 18 clients), each client is assigned images from 6, 3, or 1 city respectively, promoting spatial and semantic locality in client data. More details can be found in Appendix C.

CocoStuff, while not naturally suited to real-world federated use cases, is included to test our method’s robustness under extreme data heterogeneity. We assign each image a dominant class based on pixel-wise frequency, and apply Dirichlet sampling to partition the dataset across clients, inducing strong class imbalance and inter-client variability. More details can be found in Appendix D.

To evaluate real-world applicability, we have employed the IPS [Psarras et al., 2024] dataset, which contains high-resolution RGB images and video frames captured at four industrial sites performing pipeline infrastructure inspection. IPS poses a binary semantic segmentation task with two classes: background and pipe, and contains 984 training samples. We simulate a 3-client federation by assigning each client to a distinct site, while a fourth, unseen site is reserved exclusively for validation—assessing generalization under cross-domain deployment. Visual examples can be found in Appendix E.

## 4.2 Implementation Details

Each client is equipped with a frozen Vision Foundation Model (VFM) backbone, specifically the base version of DINO [Caron et al., 2021] pretrained on ImageNet [Russakovsky et al., 2015], which is used to extract semantically rich features from raw input images. On top of this backbone, a trainable segmentation head  $S(\cdot, \theta_S)$  is implemented as a lightweight two-layer convolutional projection network that maps the VFM 768-dimensional pixel embeddings, to a lower-dimensional embedding space of 70 dimensions.

Training of each local segmentation head  $S_k$  is performed using mini-batches of 8 query images sampled from the client’s dataset. For each query image, we select one nearest neighbor (by feature similarity) and five additional random support images from the same client. The cross-image correlation loss (Eq. 6) is computed between the query and each support image individually. We use the Adam optimizer [Kingma and Ba, 2014] with a learning rate of  $5 \times 10^{-4}$  to optimize  $\theta_{S_k}$ .

Following each local update, centroid optimization is performed by clustering the combined batch of query and support feature vectors into  $|\mathcal{C}| = 27$  clusters for Cityscapes and CocoStuff, or  $|\mathcal{C}| = 2$  for IPS. After computing the clustering loss from Eq. 5, centroids are updated using a second Adam optimizer with a learning rate of  $5 \times 10^{-3}$ .

Table 1: Experimental results comparing naive and FedCC versions of FedAvg, FedProx, and FedMoon across different client counts. Reported metric is mean Intersection-over-Union (mIoU). CRF post processing is applied to all results.

Method	Cityscapes			IPS
	3 Clients	6 Clients	18 Clients	3 Clients
FedProx	19.77	20.01	18.22	<b>84.63</b>
<b>FedProx+FedCC</b>	<b>20.96</b>	<b>20.48</b>	<b>20.90</b>	83.52
FedMOON	19.83	19.94	19.86	83.78
<b>FedMOON+FedCC</b>	<b>20.35</b>	<b>21.76</b>	<b>20.41</b>	<b>84.70</b>
FedAvg	21.12	19.94	21.25	84.10
<b>FedAvg+FedCC</b>	<b>21.83</b>	<b>21.80</b>	<b>21.53</b>	<b>84.87</b>
Centralized	21.0			85.66

All clients perform an equal number of local updates, configured to ensure that each client completes at least one full epoch over its local dataset. While the number of local steps remains fixed within each experiment, it may vary across experiments depending on available computational resources and batch size configurations. Upon completing local training, clients transmit their updated parameters

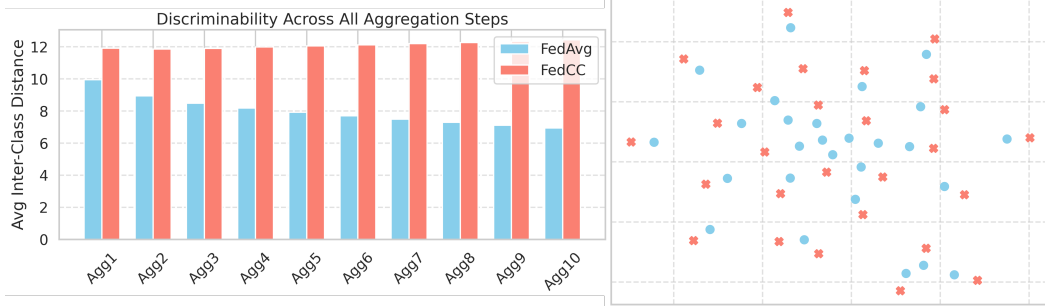


Figure 1: Left: Discriminability analysis between resulting centroids for CocoStuff non-i.i.d. Right: t-SNE projections of centroids from final federated aggregation.

to the server, which then applies one of the aggregation strategies described in Section 3.2 and broadcasts the resulting global model back to all clients.

### 4.3 Results

We evaluate FUSS on both standard benchmarks (Cityscapes) and a real-world deployment scenario (IPS), under a range of federation configurations. The primary evaluation metric is Mean Intersection-over-Union (mIoU), computed on held-out validation sets. Ground-truth labels are never used during training and serve strictly for evaluation.

To provide broader context, we also incorporate two common local training regularizers—FedProx [Li et al., 2020] and FedMoon [Li et al., 2021]—which are orthogonal to our aggregation strategies but useful for understanding FedCC’s modularity and robustness under both i.i.d. and non-i.i.d. conditions. More information about their implementation can be found at Appendix B.

Table 1 reports segmentation results for FedAvg, FedProx, and FedMoon, both with and without FedCC. Since settings remain constant across all methods and client counts, FedCC remains the only differentiating factor for the improved segmentation performance. Notably, FedAvg+FedCC achieves 21.72 mIoU on average on all federated scenarios for Cityscapes and 84.87 mIoU on IPS, closely matching centralized upper bounds. To evaluate FUSS under heterogeneous client distributions, we partition CocoStuff to 18 clients, using Dirichlet sampling ( $\alpha = 0.5$ ). Table 2 shows that FedAvg+FedCC achieves 25.39 mIoU, nearly matching the centralized score of 25.41, and outperforming both standard and FedCC-enhanced versions of FedProx and FedMoon.

Table 2: Comparison of FedCC performance, with FUSS applied to non-i.i.d (Dirichlet,  $\alpha = 0.5$ ) CocoStuff benchmark, for 18 clients.

A qualitative assessment of the results under heterogeneous data distributions is presented in Figure 1. These examples illustrate that even in strongly non-i.i.d. scenarios, the centroids produced by FedCC remain structurally discriminative across the entire federation. Furthermore, visualizations of the projected centroid embedding space reveal that while FedAvg tends to produce cluttered prototypes, FedCC maintains significantly greater inter-class separability.

To isolate the contributions of each component in FUSS, we perform an ablation study on the aggregation process—evaluating the effects of weighted averaging (W), encoder parameter fusion (E), and prototype aggregation (C). Table 3 presents results across multiclass (Cityscapes) and binary (IPS) segmentation. The aggregation module analysis confirms the benefit of explicitly aligning prototypes (C), even without encoder averaging. For instance, C-only FedAvg outperforms E-only FedAvg across the majority of settings. On IPS, FedCC-KMeans performs best, likely due to strong foreground-background separability. However, for Cityscapes—where

Method	mIoU
FedProx	22.39
FedMoon	24.69
FedAvg	24.69
FedProx + FedCC	24.38
FedMoon + FedCC	23.15
<b>FedAvg + FedCC</b>	<b>25.39</b>
Centralized	25.41



Table 3: Ablation study for multiclass (Cityscapes) and binary (IPS) federated unsupervised semantic segmentation. We evaluate the impact of three aggregation modules: W = weighted averaging (by client dataset size), E = encoder aggregation, C = centroid aggregation. Reported scores are mean Intersection-over-Union (mIoU). For configurations with no resulting global model, we report the average result along with the best and worst-performing clients.

Method	Agg. Modules			Cityscapes			IPS
	W	E	C	3 Clients	6 Clients	18 Clients	3 Clients
No Agg.				18.60 <sup>+0.72</sup> <sub>-0.69</sub>	18.20 <sup>+1.07</sup> <sub>-1.62</sub>	16.74 <sup>+1.71</sup> <sub>-1.62</sub>	67.24 <sup>+15.0</sup> <sub>-27.0</sub>
FedAvg		✓		18.55 <sup>+0.6</sup> <sub>-0.7</sub>	17.97 <sup>+0.72</sup> <sub>-0.48</sub>	17.18 <sup>+1.52</sup> <sub>-1.58</sub>	70.74 <sup>+12.4</sup> <sub>-18.0</sub>
			✓	19.91 <sup>+0.24</sup> <sub>-0.15</sub>	18.11 <sup>+0.74</sup> <sub>-0.61</sub>	16.46 <sup>+0.90</sup> <sub>-1.17</sub>	80.88 <sup>+2.9</sup> <sub>-2.4</sub>
		✓	✓	19.26	18.22	17.55	80.64
	✓	✓		18.55 <sup>+0.7</sup> <sub>-0.7</sub>	18.45 <sup>+0.47</sup> <sub>-1.22</sub>	17.36 <sup>+1.42</sup> <sub>-2.20</sub>	78.43 <sup>+4.78</sup> <sub>-4.73</sub>
	✓		✓	18.69 <sup>+0.60</sup> <sub>-0.59</sub>	17.98 <sup>+0.63</sup> <sub>-0.85</sub>	16.51 <sup>+0.99</sup> <sub>-1.14</sub>	79.10 <sup>+1.3</sup> <sub>-1.1</sub>
	✓	✓	✓	19.24	18.96	17.50	79.16
FedCC — kmeans			✓	18.91 <sup>+0.67</sup> <sub>-0.86</sub>	18.90 <sup>+0.66</sup> <sub>-0.83</sub>	17.35 <sup>+1.1</sup> <sub>-1.4</sub>	81.14 <sup>+2.76</sup> <sub>-2.07</sub>
	✓		✓	18.61 <sup>+0.33</sup> <sub>-0.55</sub>	18.59 <sup>+0.33</sup> <sub>-0.60</sub>	17.50 <sup>+1.0</sup> <sub>-1.1</sub>	79.49 <sup>+1.29</sup> <sub>-1.11</sub>
		✓	✓	18.88	19.41	17.89	80.67
	✓	✓	✓	<b>19.71</b>	19.39	17.87	<b>82.60</b>
FedCC — maximin			✓	18.51 <sup>+0.11</sup> <sub>-0.08</sub>	18.90 <sup>+0.66</sup> <sub>-0.83</sub>	17.06 <sup>+1.26</sup> <sub>-1.45</sub>	81.01 <sup>+2.9</sup> <sub>-1.65</sub>
	✓		✓	19.06 <sup>+0.22</sup> <sub>-0.45</sub>	18.57 <sup>+0.56</sup> <sub>-0.55</sub>	17.54 <sup>+0.9</sup> <sub>-1.2</sub>	79.43 <sup>+1.5</sup> <sub>-1.4</sub>
		✓	✓	19.50	19.38	18.12	78.22
	✓	✓	✓	<u>19.52</u>	<b>19.64</b>	<b>18.87</b>	80.27

small objects and semantic clutter dominate—FedCC-Maximin proves more effective by promoting inter-centroid diversity and mitigating prototype collapse.

Together, our results demonstrate that FUSS enables accurate, decentralized segmentation with minimal communication, and that our aggregation strategies scale across dataset complexities and federation settings.

## Limitations

Despite its practical value, FUSS inherits key limitations from the USS paradigm. Most notably, it assumes a fixed number of semantic regions  $|\mathcal{C}|$  across all clients, regardless of local content. This may lead to over-clustering in simpler clients or under-representation of fine-grained classes in complex ones. Additionally, following common FL conventions, our encoder aggregation relies on simple weighted averaging, without taking into account local model quality or encoding variance. Future work could explore adaptive strategies based on representation diversity or cluster coherence.

Finally, while we simulate non-i.i.d. settings using spatial splits (Cityscapes) and Dirichlet sampling (CocoStuff), the lack of a standardized protocol for inducing heterogeneity in unsupervised segmentation remains an open problem. Defining realistic, benchmarkable heterogeneity scenarios is an important direction to evaluate federated USS frameworks more rigorously.

## 5 Conclusion

This work introduced **FUSS**, a Federated Unsupervised image Semantic Segmentation framework designed for decentralized, label-free semantic image segmentation under strict data privacy constraints. FUSS builds upon recent advances in self-supervised vision foundation models and clustering-based optimization to enable collaborative semantic segmentation without the need for ground-truth annotations or data sharing.

We addressed a critical gap in existing federated learning literature by proposing a general formulation that integrates unsupervised representation learning with class prototype alignment across clients. Through a combination of correlation-based local optimization and novel aggregation

strategies—including variations of weighted parameter averaging and global clustering procedures—we demonstrated that FUSS effectively mitigates challenges such, semantic misalignment, and local overfitting.

Extensive experiments on both benchmark (Cityscapes, CocoStuff) and real-world (IPS) datasets show that our method consistently outperforms local-only and traditional Federated Learning training baselines, achieving segmentation quality competitive with centralized unsupervised models, while remaining scalable and robust in i.i.d and non-i.i.d data regimes.

Future extensions may explore end-to-end learnable aggregation schemes, adaptive client weighting strategies based on local task uncertainty, or integration with semi-supervised constraints when limited labels become available.

## References

- H. Caesar, J. Uijlings, and V. Ferrari. Coco-stuff: Thing and stuff classes in context. In *IEEE/CVF Conference on Computer Vision and Pattern Recognition (CVPR)*, pages 1209–1218, 2018.
- D. Caldarola, B. Caputo, and M. Ciccone. Improving generalization in federated learning by seeking flat minima. In *European Conference on Computer Vision (ECCV)*, pages 654–672. Springer, 2022.
- M. Caron, H. Touvron, I. Misra, H. Jégou, J. Mairal, P. Bojanowski, and A. Joulin. Emerging properties in self-supervised vision transformers. In *IEEE/CVF International Conference on Computer Vision (ICCV)*, pages 9650–9660, 2021.
- J. Chen, B. Ma, H. Cui, and Y. Xia. Think twice before selection: Federated evidential active learning for medical image analysis with domain shifts. In *IEEE/CVF Conference on Computer Vision and Pattern Recognition (CVPR)*, pages 11439–11449, 2024.
- M. Cordts, M. Omran, S. Ramos, T. Rehfeld, M. Enzweiler, R. Benenson, U. Franke, S. Roth, and B. Schiele. The cityscapes dataset for semantic urban scene understanding. In *IEEE/CVF Conference on Computer Vision and Pattern Recognition (CVPR)*, 2016.
- A. Dosovitskiy, L. Beyer, A. Kolesnikov, D. Weissenborn, X. Zhai, T. Unterthiner, M. Dehghani, M. Minderer, G. Heigold, S. Gelly, et al. An image is worth 16x16 words: Transformers for image recognition at scale. In *International Conference on Learning Representations (ICLR)*, 2020.
- L. Fantauzzo, E. Fanì, D. Caldarola, A. Tavera, F. Cermelli, M. Ciccone, and B. Caputo. Feddrive: Generalizing federated learning to semantic segmentation in autonomous driving. In *IEEE/RSJ International Conference on Intelligent Robots and Systems (IROS)*, pages 11504–11511. IEEE, 2022.
- X. Gong, A. Sharma, S. Karanam, Z. Wu, T. Chen, D. Doermann, and A. Innanje. Ensemble attention distillation for privacy-preserving federated learning. In *IEEE/CVF International Conference on Computer Vision (ICCV)*, pages 15076–15086, 2021.
- B. Guermazi, R. Ksantini, and N. Khan. Dynaseg: A deep dynamic fusion method for unsupervised image segmentation incorporating feature similarity and spatial continuity. *Image and Vision Computing*, 150:105206, 2024.
- M. Hamilton, Z. Zhang, B. Hariharan, N. Snavely, and W. T. Freeman. Unsupervised semantic segmentation by distilling feature correspondences. In *International Conference on Learning Representations*, 2022.
- K. He, X. Zhang, S. Ren, and J. Sun. Deep residual learning for image recognition. In *IEEE/CVF Conference on Computer Vision and Pattern Recognition (CVPR)*, pages 770–778, 2016.
- C. Kim, W. Han, D. Ju, and S. J. Hwang. Eagle: Eigen aggregation learning for object-centric unsupervised semantic segmentation. In *IEEE/CVF Conference on Computer Vision and Pattern Recognition (CVPR)*, pages 3523–3533, 2024.
- D. P. Kingma and J. Ba. Adam: A method for stochastic optimization. *arXiv preprint arXiv:1412.6980*, 2014.

- Q. Li, B. He, and D. Song. Model-contrastive federated learning. In *IEEE/CVF Conference on Computer Vision and Pattern Recognition (CVPR)*, pages 10713–10722, 2021.
- T. Li, A. K. Sahu, M. Zaheer, M. Sanjabi, A. Talwalkar, and V. Smith. Federated optimization in heterogeneous networks. *Proceedings of Machine learning and systems*, 2:429–450, 2020.
- X. Liao, W. Liu, C. Chen, P. Zhou, F. Yu, H. Zhu, B. Yao, T. Wang, X. Zheng, and Y. Tan. Rethinking the representation in federated unsupervised learning with non-iid data. In *IEEE/CVF Conference on Computer Vision and Pattern Recognition (CVPR)*, pages 22841–22850, 2024.
- E. Lubana, C. I. Tang, F. Kawsar, R. Dick, and A. Mathur. Orchestra: Unsupervised federated learning via globally consistent clustering. In *International Conference on Machine Learning (ICML)*, pages 14461–14484. PMLR, 2022.
- J. MacQueen. Some methods for classification and analysis of multivariate observations. In *Fifth Berkeley Symposium on Mathematical Statistics and Probability, Volume 1: Statistics*, volume 5, pages 281–298. University of California press, 1967.
- B. McMahan, E. Moore, D. Ramage, S. Hampson, and B. A. y Arcas. Communication-efficient learning of deep networks from decentralized data. In *Artificial Intelligence and Statistics*, pages 1273–1282. PMLR, 2017.
- J. Miao, Z. Yang, L. Fan, and Y. Yang. Fedseg: Class-heterogeneous federated learning for semantic segmentation. In *IEEE/CVF Conference on Computer Vision and Pattern Recognition (CVPR)*, pages 8042–8052, 2023.
- D. Psarras, C. Papaioannidis, V. Mygdalis, and I. Pitas. A unified dnn-based system for industrial pipeline segmentation. In *IEEE International Conference on Acoustics, Speech and Signal Processing (ICASSP)*, pages 7785–7789. IEEE, 2024.
- O. Russakovsky, J. Deng, H. Su, J. Krause, S. Satheesh, S. Ma, Z. Huang, A. Karpathy, A. Khosla, M. Bernstein, et al. Imagenet large scale visual recognition challenge. *International journal of computer vision*, 115:211–252, 2015.
- Y. Tang, C. Zhao, J. Wang, C. Zhang, Q. Sun, W. X. Zheng, W. Du, F. Qian, and J. Kurths. Perception and navigation in autonomous systems in the era of learning: A survey. *IEEE Transactions on Neural Networks and Learning Systems*, 34(12):9604–9624, 2022.
- H. Wang, X. Liu, J. Niu, W. Guo, and S. Tang. Why go full? elevating federated learning through partial network updates. In *Neural Information Processing Systems (NeurIPS)*, 2024.

## A FUSS framework visualization

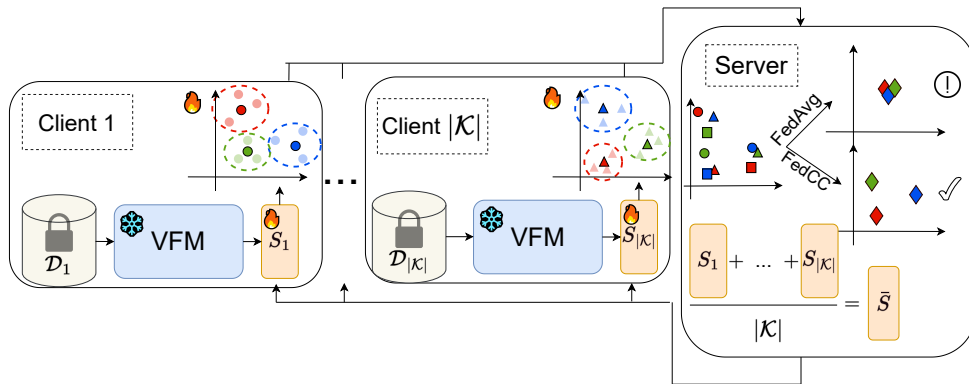


Figure 2: Overview of the proposed FUSS framework.

Figure 2 provides a visual overview of the proposed **FUSS** framework, as described in Section 3. Each client performs local unsupervised training using self-supervised objectives and periodically

transmits its learned segmentation head and semantic prototypes to a central server. The server aggregates these parameters and broadcasts the updated global model back to all clients.

While traditional federated strategies may result in disorganized or overlapping class prototypes due to local heterogeneity, our proposed aggregation methods explicitly promote semantic alignment and prototype separability across the federation.

## B Client-Side Regularization Baselines

**FedProx.** FedProx [Li et al., 2020] adds a proximal term to the local loss to prevent divergence from the global model under non-i.i.d. data. In FUSS, we apply it to the segmentation head:

$$\mathcal{L}_{\text{FedProx}} = \mathcal{L}_{\text{local}} + \frac{\mu}{2} \|\theta_{S_k} - \bar{\theta}_S\|^2,$$

where  $\mu$  controls regularization strength. Since encoders are frozen and centroids are directly aggregated, only the segmentation head is regularized.

**FedMoon.** FedMoon [Li et al., 2021] introduces a contrastive loss to align local and global representations. In FUSS, we apply this to the segmentation embeddings:

$$\mathcal{L}_{\text{Moon}} = -\log \left( \frac{\exp(s_{\text{cos}}(\mathbf{z}_k, \bar{\mathbf{z}})/\tau)}{\exp(s_{\text{cos}}(\mathbf{z}_k, \bar{\mathbf{z}})/\tau) + \exp(s_{\text{cos}}(\mathbf{z}_k, \mathbf{z}_k^{\text{prev}})/\tau)} \right),$$

and define the final objective as  $\mathcal{L}_{\text{FedMoon}} = \mathcal{L}_{\text{local}} + \lambda \cdot \mathcal{L}_{\text{Moon}}$ . This promotes representation consistency across rounds.

## C Cityscapes Federation Scenarios

Table 4: Example of Cityscapes split for applied federation scenarios

City	Configurations		
	3 clients	6 clients	18 clients
aachen	client 1	client 1	client 1
bochum			client 2
bremen			client 3
cologne		client 2	client 4
darmstadt			client 5
dusseldorf			client 6
erfurt	client 2	client 3	client 7
hamburg			client 8
hanover			client 9
jena		client 4	client 10
krefeld			client 11
monchengladbach			client 12
stuttgart	client 3	client 5	client 13
strasbourg			client 14
tubingen			client 15
ulm		client 6	client 16
weimar			client 17
zurich			client 18

Each federation client  $k$  receives a disjoint subset  $\mathcal{D}_k$  composed of images from geographically distinct cities, introducing domain distribution shifts. An example of the Cityscapes split for each

federation simulation can be observed in Table 4. We also apply a five-crop on each image as a data augmentation technique, to better handle training times and small objects.

### C.1 Cityscapes qualitative results



Figure 3: Visual representation Cityscapes results. **Top:** Sample validation images. **Top-Middle:** Corresponding ground-truth binary segmentation masks. **Bottom-Middle:** FedAvg FUSF results. **Bottom:** FedCC FUSF results.

## D CocoStuff non-i.i.d Sampling

We construct non-i.i.d. partitions of the COCO-Stuff dataset using a Dirichlet-based sampling strategy informed by semantic supercategories. The process involves assigning each image to a single coarse semantic class based on pixel frequency, followed by Dirichlet sampling to allocate images to clients in a skewed but controllable manner.

### Dominant Supercategory Assignment

Each COCO-Stuff image is annotated with a pixel-wise segmentation mask covering 182 fine-grained classes. To facilitate class-conditional sampling, we assign a single coarse label to each image based on the most frequently occurring supercategory. Let  $\mathbf{Y}' \in \mathbb{R}^{H \times W}$  be the RGB fine-grained segmentation mask of an image  $\mathbf{X}$ , and let  $f : \mathcal{C}_{\text{fine}} \rightarrow \mathcal{C}_{\text{coarse}}$  be a known mapping from the 182 fine-grained to the 27 coarse classes that we use in our experiments, following common USS conventions. The dominant coarse label for image  $\mathbf{X}$  is defined as:

$$\hat{c} = \arg \max_{c \in \mathcal{C}_{\text{coarse}}} \left| \left\{ (h, w) \mid f\left(\mathbf{Y}'^{(h, w)}\right) = c \right\} \right|,$$

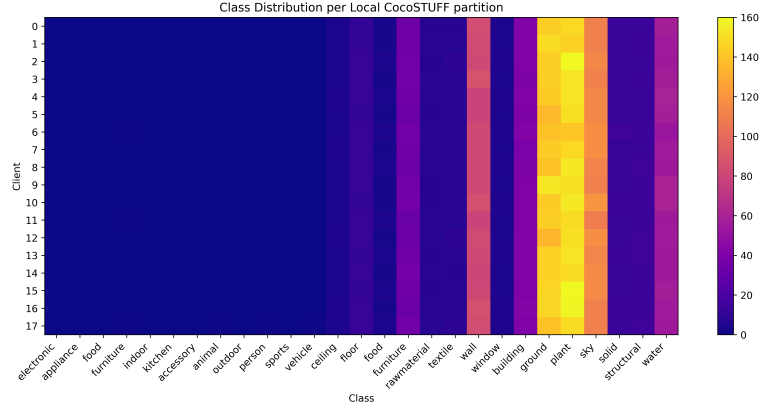
i.e., the supercategory  $\hat{c}$  that occurs most frequently across all pixels of the image. Each image is thus labeled with a single dominant supercategory, enabling label-driven data partitioning despite the absence of ground-truth image-level annotations.

### Dirichlet Client Assignment

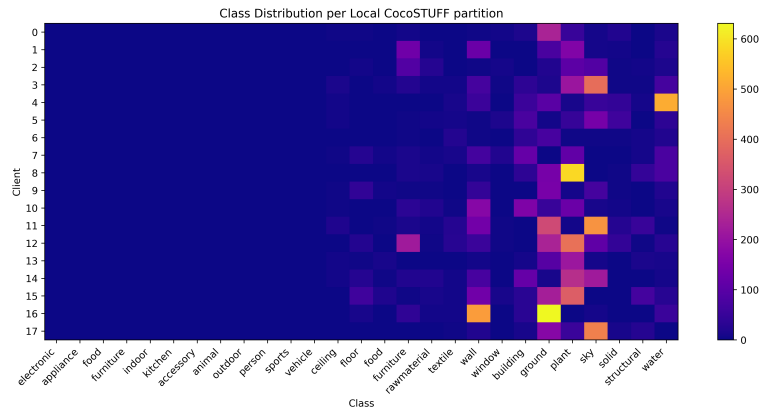
Once each image is tagged with its dominant coarse category, we simulate heterogeneous federated settings by partitioning the data using Dirichlet sampling over coarse class distributions. Specifically, for  $K$  clients and a Dirichlet concentration parameter  $\alpha$ , we draw a probability vector  $\mathbf{p}_c \sim \text{Dir}(\alpha \cdot \mathbf{1}_K)$  for each supercategory  $c \in \mathcal{C}_{\text{coarse}}$ . This vector determines the probability that an image with dominant category  $c$  is assigned to each client.

Images are then distributed across clients accordingly. Lower values of  $\alpha$  (e.g., 0.5) induce higher heterogeneity by skewing the distribution of dominant classes across clients, while larger  $\alpha$  values produce more balanced partitions. In Figure 4, we provide a visual comparison of prototype alignment under both i.i.d. and non-i.i.d. client distributions.

This approach ensures that each client receives a diverse but biased subset of the full dataset, approximating realistic non-i.i.d. scenarios in federated learning while retaining control over the degree of distributional shift.



(a)



(b)

Figure 4: A CocoStuff split visualization for 18 clients, based on dominant class frequency. (a) i.i.d., (b) non-i.i.d, with Dirichlet concentration parameter  $\alpha = 0.5$

## E Industrial Pipeline Segmentation Dataset

Figure 5 provides a visual overview of Industrial Pipeline Segmentation (IPS) samples, originally introduced in [Psarras et al., 2024].

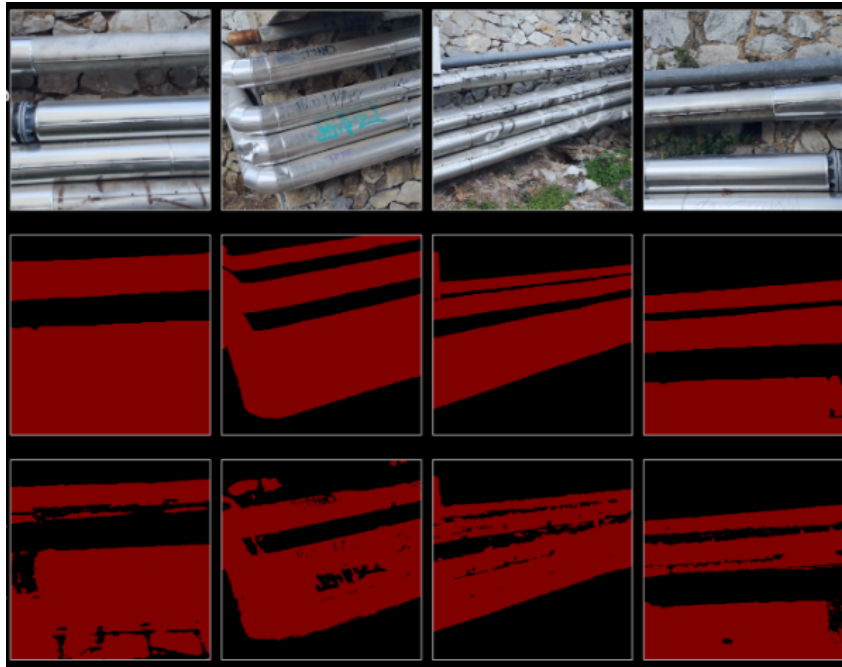


Figure 5: Visual representation of the IPS dataset. **Top:** Sample validation images. **Middle:** Corresponding ground-truth binary segmentation masks. **Bottom:** Predicted masks produced by FUSS with FedCC (k-means) aggregation.